DESIGN STUDY RELATING TO AXIAL FLOW FAN STATOR BLADE ROW USED IN REVERSE VENTILATION

Vaclav CYRUS, Jan CYRUS

AHT Energetika Ltd., Podnikatelska 550,
190 11 Prague-Bechovice, Czech Republic

SUMMARY

Fan flow directional change is frequently required in ventilation systems during emergencies in traffic tunnels, coalmines or chemical plants. Flow reversal is usually carried out by changing the direction of rotation and by turning the stator vanes, which must have the capability of turning in one go around their axis. New stator vanes were designed for two axial fan Stages A and B, with different cascade aerodynamic loading. Stage A with moderate loading of the stator cascade can use vanes that rotate around their axis and with the cascade spacing and chord ratio s/c greater than 1.0 along the radius. Stage B with higher aerodynamic loading has stator vanes consisting of two parts, namely straight part that is fixed and curved part that is moveable.

INTRODUCTION

Fan flow directional change is often required in ventilation systems during emergencies in traffic tunnels, coalmines or miscellaneous chemical plants' production lines. Axial flow fans consisting of a rotor blade row, an inlet guide and stator vane rows (Fig. 1) are used. The flow reversal is usually carried out by changing the direction of rotation and by turning the stator vanes. The other flow reversing method is by turning the fan rotor blades during the operational run.

The required reverse flow rate Q_{rev} is typically at least 60 % of the standard working rate Q_n. The stage blading efficiency $\eta_{,max}$ should be higher than 89 % to 90 % for the standard operational run. Fan efficiency η_{rev} is not usually prescribed in emergencies. Companies that procure axial fans require that the stator vanes will have the capability of turning in one go around their axis in emergency events to enable the reverse flow.

Literature references to 3D reverse flow in axial fans that is produced by changing the direction of rotation may only be found in publications by Brusilovskij [1] and Cyrus [2]. These fan stages have low aerodynamic loading of the blade rows elements at the standard flow conditions.

Contribution to understanding the flow mechanism in axial flow fans during the flow reversal by turning the rotor blades may be found in more detail in the paper by Cyrus et al [3]. The turning is carried out by the tailor-made blade mechanism that uses gears. Better flow aerodynamic performance was found in the axial fan that uses the flow reversing method by turning the rotor blades. The two above-mentioned methods of reversing the flow were compared in the said paper [3] using the reliability and costs parameters.

Our paper presents the study of the stator blades design used in the reversing method where the directional change of rotation and turning of the stator vanes in one go is carried out. New stator vanes were designed for the two axial fan stages, namely A and B, with different cascade aerodynamic loading. The stage with moderate loading of the stator cascade can use vanes that turn around their axis, where the cascade spacing and chord ratio s/c is greater than 1.0 along the full span. In the event that the higher fan loading is required, special vanes designed by authors may be used. The stator vanes consist of two parts, fixed straight part and movable curved part; parts are connected during the standard flow. For the reverse flow, the moveable curved stator blade is turned to ensure the maximum flow rate. Effect of the stator vane design options for turning in one go (reversing) on the fan performance was investigated in relation to the Stage A and B efficiency computed with the use of flow simulation data.

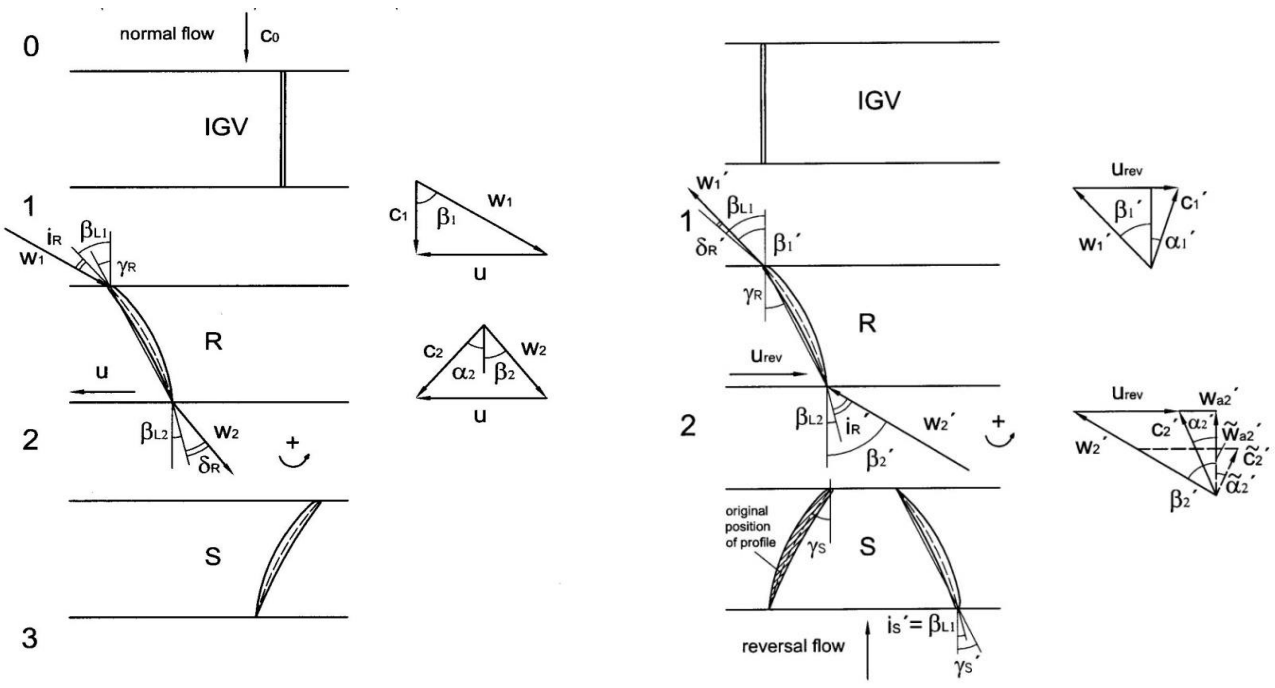

Figure 1: Diagrams of reverse axial flow stage with velocity triangles

AXIAL STAGES A AND B

Our paper examines data relating to two ventilation axial fan flow stages, denoted A and B, designed by AHT Energetika with the aid of in-house design code designated for the axial flow compressor stages [7]. Selected key aerodynamic and geometric parameters are given in Table 1. Stage A has moderate aerodynamic loading, which is suitable for most ventilation fans. Blade

geometry is given at the mean radius r_m ($r_m = 0.5\ (r_t + r_h)$). Stage parameters φ and ψ are defined by equations (1) and (2) in the following chapter.Quantity *z* denotes number of blades. The cascade profile camber υ is expressed by the following relationship : $\upsilon = \beta_{L1} - \beta_{L2}$, where β_{L1} and β_{L2} are blade angles. The hub/tip ratio is defined as follows $\nu = r_h/r_t$. $D_{R,m}$ is the design diffusion factor of the rotor blade elements on the mean radius, originally formulated by Lieblein [4].

Stage external and internal diameters were constant with 600 mm external diameter consisting of the rotor and stator rows and the inlet guide vanes (Fig. 1). Rotor profiles (Stages A and B) and stator (Stage A) airfoils were NACA 65 series with reinforced trailing edge and circular camber lines.

Stage B with higher aerodynamic loading had curved plate stator vanes. Vane circular camber line had constant radius along the vane height. The inlet blade angle β_{L1} was changed in the radial direction by using the chord length.

Blades were designed assuming the uniform spanwise work distribution. Relative radial clearance between the rotor blade tip and the casing was not constant along the stage axis. Near the rotor blade axis the ratio of tip clearance and chord length s_r/c was 0.008. At the leading and trailing edges, the radial clearance was greater, namely $s_r/c = 0.018$ to enable the rotor blade turning.

Table 1: Fan stage design parameters

Stage	Design parameters									
	φ_D	ψ_D	D_{Rm}	ν	z_R	z_S	$\upsilon_{R,m}$ (°)	$\upsilon_{S,m}$ (°)	$(s/c)_{S,h}$	$(s/c)_{S,t}$
A	0.40	0.30	0.36	0.55	12	15	19.5	45.0	0.86	1.85
B	0.35	0.42	0.48	0.63	16	17	24.6	51,1	0.56	0.89

Test procedure

Tests were carried out at 1,500 rpm with the inlet flow Mach number lower than 0.35. The Reynolds number $Re = u_t\, c_{R,m}\, /\nu$ varied within the range of 300,000 to 450,000, where ν is air kinematic viscosity and $c_{R,m}$ is rotor blade length at mid-span.

Test rig was fitted with the inlet measuring nozzle to indicate the mass flow rate. Radial diffuser was located at the outlet whose moveable rear wall made it possible to change the aerodynamic resistance. The rig was driven by a DC motor with a swinging stator to measure torque by weighing. The absolute measurement uncertainty of the stage efficiency was calculated as ± (0.9 % to 1.1 %).

Numeric simulations

FINE™/Turbo Numeca Code [8] solved the full Reynolds-averaged Navier-Stokes equations (RANS equations) on the structured multi-block arbitrary grid topologies with mixing planes between the adjacent blade rows. The Spallart-Almaras turbulence model was used. All blade rows were modelled using the standard elliptical H-grid. Clearance gaps were solved by using a separate grid block of approximately 30,000 points. The overall mesh size relating to the fan blading was approximately 800,000 – 1,000,000 points for a complete stage with y+ values smaller than 5.

Convergence was evaluated through the computation of residuals, which at the end of calculations were of the order 10^{-6}. The convergence of the stage efficiency was also considered. The difference in the stage efficiency during the last iterations did not exceed 0.05 % to 0.1 %. Operating points were modelled by changing the static backpressure.

REVERSE FLOW ANALYSIS

2D standard fan stage cascades together with the velocity triangles valid for the reverse run are shown in Fig. 1. By changing the direction of rotation of the rotor blade row the compressor type cascade becomes the turbine type cascade. The relative flow angles should be $\beta'_2 > \beta'_1$ for the compressor regime of cascade in the reverse run. This is caused by the flow separation area on the blade's pressure surface.

The stator vanes were rearranged in the opposite sense of the stagger angle γ_S with respect to the original position, as it follows from the velocity triangle in the Plane 2. If we wished to achieve the same relative flow angle β'_2 and thus also the incidence angle of the rotor row i'_R whilst keeping the original stator stagger angle adjustment, we would have to significantly decrease the axial velocity component $\tilde{w}'_{a2}$, as it follows from the velocity triangle. However, this is not desirable, because it increases the difference between the axial flow stage characteristics for the standard and reverse run [2]. The main fan stage parameters, namely the flow coefficient φ, pressure coefficient ψ and efficiency η are defined as follows:

$$\varphi = Q/(A) \tag{1}$$

$$\psi = 2\,\Delta p_T/\rho\, u_t^2 \tag{2}$$

$$\eta = Q\,\Delta p_T/P \tag{3}$$

Where A is the flow area $A = \pi\, D_t^2/4\,(1 - \nu^2)$; u_t is peripheral velocity; Δp_T is total pressure increment in the fan stage; ρ is gas density; D_t is external diameter; ν is stage hub/tip ratio and P is the fan stage work input.

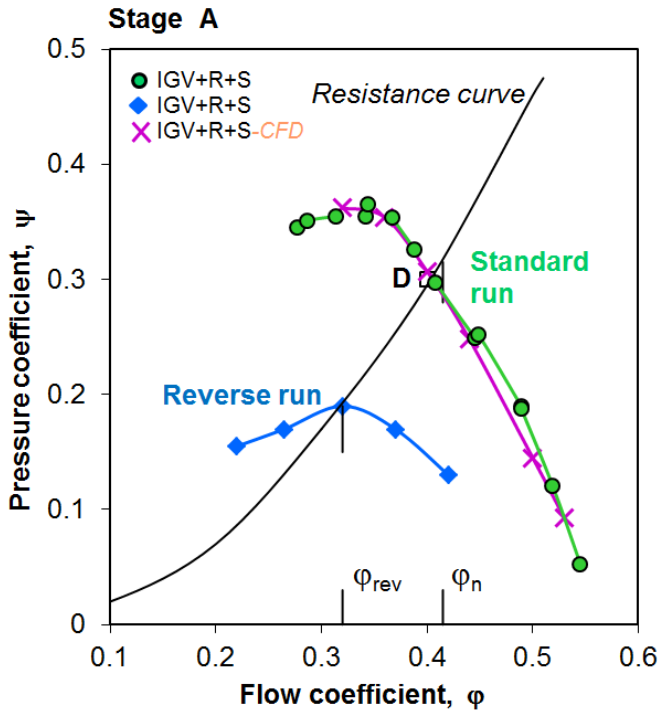

Figure 2: Stage A measured and computed aerodynamic performance

Comparison of the Fan stage A measured and computed pressure coefficient ψ and flow coefficient φ graphs for the standard and reverse run is shown in Fig. 2. The stator vanes were set to the stagger angle of $\gamma_S = -10^o$ at flow reversal. The resistance curve shown in the said figure intersects the design point D. Measured flow coefficients ratio φ_{rev}/φ_n is 0.77. Stage B ratio is lower,

i.e. $\varphi_{rev}/\varphi_n = 0.62$ owing to the higher aerodynamic loading of the rotor blade elements. Comparison of the measured and computed performance for the standard Fan A run is acceptable (Fig. 2). However, the comparison is not satisfactory for the reverse flow. This relates to the occurrence of large areas of separated flow in the rotor blade row and the inlet guide vanes; consequently the results are not presented.

DESIGN OF TURNING STATOR VANES FOR REVERSE AXIAL FANS

High efficiency ventilation axial fan stages are usually designed according to the free-vortex law with the constant spanwise distribution of work, axial velocity and total air pressure; refer to [5]. This results in the largest inlet stator absolute flow angle at the stage hub with the pitch/chord ratio of the stator blade row being less than the limit, i.e. s/c < 1.0. In such case, the stator vanes should be turned gradually in two or three steps. This is not acceptable in emergencies, as mentioned above.

Companies that procure reverse axial fans require that the stator vanes will have the capability of turning in one go around their axis in emergency events to enable the reverse flow; refer to the preceding text. Accordingly, the stator blade cascade should have higher pitch/chord ratio than one, namely s/c > 1.0 along the full blade span. New stator vane shape for the reverse fan is characterised by the decrease in the chord length, in the radial direction to the fan axis. Consequently, the cascade aerodynamic loading increases when compared with the original stage design. This is only possible if the aerodynamic loading of blade cascade is moderate. The cascade aerodynamic loading is frequently given by the Lieblein's definition of the diffusion factor D [4]:

$$D = 1 - \cos \alpha_2/\cos \alpha_3 + 0.5\ s/c\ (\mathrm{tg}\ \alpha_2 - \mathrm{tg}\ \alpha_3) \cos \alpha_3 \qquad (4)$$

Meaning of variables is given in Fig. 1. If the diffusion factor is D > 0.60 then the flow is separated on the cascade's profile suction surface.

Chord length of the turning stator vane should be decreased where the pitch/chord ratio s/c is less than 1.02, thus ensuring that the vane turns around its axis. We may recap that the vane axis is going through a particular vane profiles centroid.

It is assumed that the axial flow at the stator row has the exit plane angle $\alpha_3 = 0^o$ and consequently the relationship (4) may be written as follows:

$$D = 1 - \cos \alpha_2 + 1/2\ s/c \sin \alpha_2 \qquad (5)$$

Graph of the diffusion factor D, calculated using equation (4), against the stator inlet flow angle is plotted in Fig. 3 with the pitch/chord ratio s/c = 1.02. The diffusion factor's critical limit, i.e. D = 0.6 is also plotted.

The inlet flow angle limit $\alpha_2 = 40^o$ was obtained for D = 0.56 in our design study and this is the reason why the large flow separation area should not occur in the stator vane cascade. Some data on the origin of separated flow in four low speed axial compressor stages may be found in [6].

The total pressure increase in the fan stage can be determined according to the Euler equation, e.g. [5] valid for incompressible flow:

$$\Delta p_c = \eta\ \rho\ u\ w_{u2} \qquad (6)$$

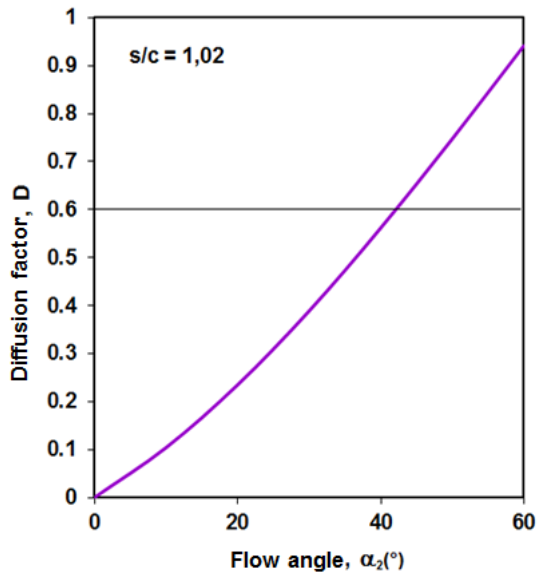

Figure 3: Diffusion factor and cascade inlet angle

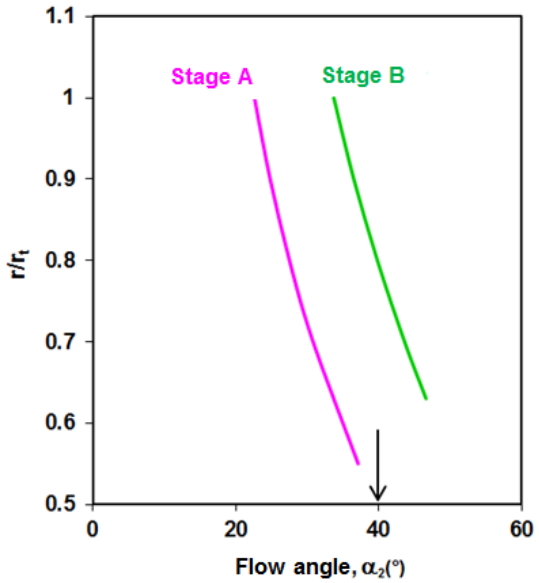

Fig. 4: Stage A and B inlet flow angle spanwise distribution

Where w_{u2} is the peripheral component of the absolute velocity at the rotor blade row's outlet and η is the stage efficiency.

If the stage blading was designed in accordance with the free-vortex law, the following equation may be derived with the use of the pressure coefficient ψ and flow coefficient φ definitions:

$$\alpha_2 = \arctan\left(\frac{1}{2\eta}\frac{\psi}{\varphi}\frac{r_t}{r}\right). \tag{7}$$

Typical stage efficiency η = 0.9 was used for the design condition.
Graphs of the stator inlet flow angle α_2 against the relative stage radius r/r_t are shown for the Stage A and B in Fig. 4. It is evident that the inlet flow angle α_2 increases with the increase of the pressure coefficient ψ, and with the decrease of the flow coefficient φ and ratio r/r_t. The largest stator inlet flow angle is on the fan's hub. It can be deduced from Fig. 4 that the design of turning stator vanes for the Stage A is feasible for the reverse flow with the inlet flow angle on the hub being $\alpha_2 = 37^o$.

However, in analysing the Stage B we found that the inlet flow angle of the stator vane row $\alpha_2 = 47^o$ is above the critical limit in the lower half of annulus height near the fan hub. This condition would cause large flow separation area together with unacceptable decrease in the fan efficiency.

STAGE A STATOR VANE DESIGN

New turning stator vanes were designed with the aid of in-house design code designated for the axial flow compressor stages [7]. The stator vane airfoils were NACA 65 series with reinforced trailing edge.

The newly designed Stage A stator vane parameters, denoted in red, are compared with the original stator vane parameters, denoted in blue, in Figs. 5, 6 and 7.

New stator vane profile for the reverse fan is characterised by the decrease in the chord length and pitch/chord ratio s/c, in the radial direction to the fan axis. New blade row s/c ratio equals to 1.02 at the stage hub, consequently the cascade aerodynamic loading D and camber υ increases in this region when compared with the original stage design. At casing, the pitch/chord ratio s/c is the same as for the original stator vane row.

Comparison of the Stage A computed aerodynamic performance, for the standard run, between the original and new turning stator vanes row was carried out using the commercial flow simulation code data [8]. The difference between the stage efficiencies $\Delta\eta = \eta_{orig} - \eta_{new,rot}$ was within the range of 0.5 % to 1.5 %, if the flow coefficient φ was within the range of 0.36 to 0.50. At the design point, i.e. φ = 0.40, the difference between the stage efficiencies was found to be $\Delta\eta$ = 0.5 %. Acquired results may be assessed as relatively good.

STAGE B STATOR VANE DESIGN

Standard stator vane

Stage B original stator vanes were made from curved plate; the stator row had relatively low pitch/chord ratio s/c in its lower section, i.e. $(s/c)_{S,h}$ = 0.56; refer to Table 1. In consequence, new stator vane was designed [9], consisting of two parts, fixed straight part and moveable curved part; the said parts are connected during the standard flow. During the reverse flow, the moveable curved stator blade part is turned to ensure the maximum flow rate; refer to Fig. 8. Length of the curved part c_{S1} = 59.5 mm and of the straight part c_{S2} = 75.0 at the mid-span as shown in Fig. 8. New standard stator vane is designated as Va. It could be added that the original vane length was $c_{S,orig}$ = 125 mm along the radius. Comparison of the original Stage B aerodynamic performance acquired in tests and the stage with new stator vanes (CFD) is presented in Fig. 9. The decrease in the stage efficiency ($\Delta\eta = \eta_{orig,exp} - \eta_{new,Va}$) was found to be between 0.6 % and 1.9 % along the performance graph within the flow coefficient's φ range of 0.3 to 0.48; $\Delta\eta$ was 1.2 % at the design point. The comparison outcome is acceptable.

The spanwise distribution of the stator row's averaged outlet flow angle α_3 with the new vanes Va is shown in Fig. 10. The maximum flow deviation from the axial direction is 2.5° in the annulus area outside the end-wall boundary layers, which does not adversely affect the fan's outlet diffuser performance.

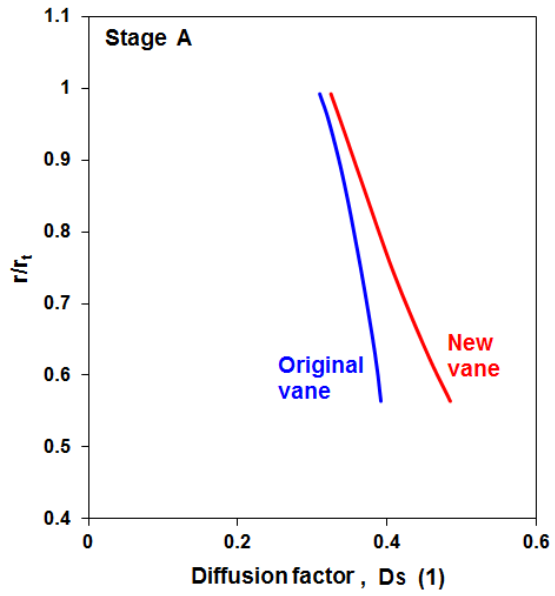

Figure 5:Spanwise distributions of the stator diffusion factor

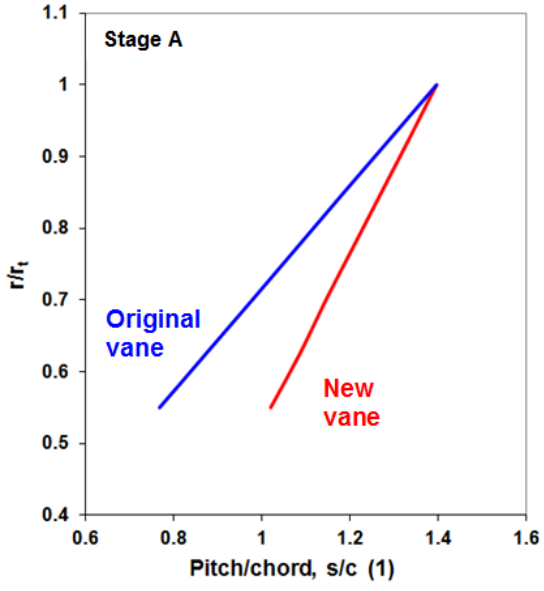

Fig 6: Spanwise distributions of the stator pitch/chord ratio

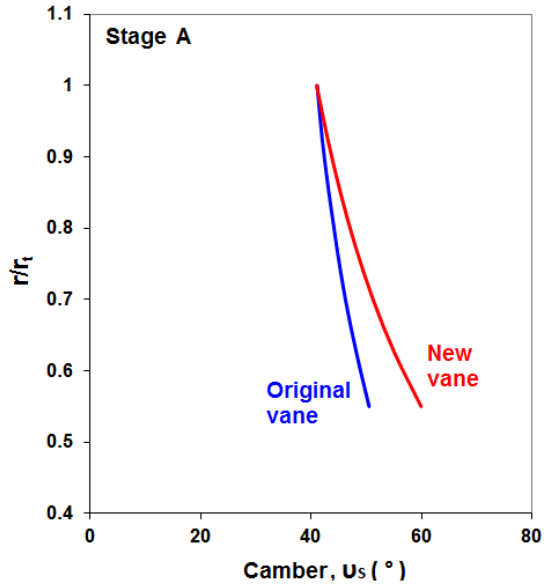

Figure 7: Spanwise distributions of the stator camber angle

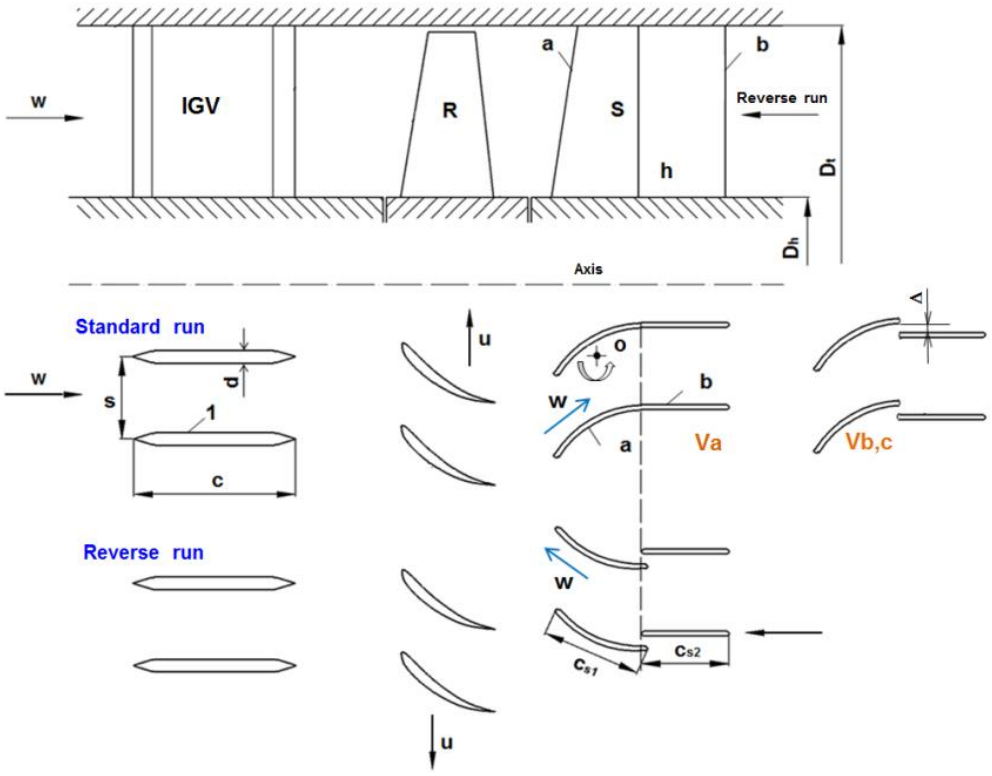

Figure 8: Diagram showing reverse axial flow fan stage with stator vanes consisting of two parts

The total loss coefficient for the stator row with the original re-staggered (γ_S = -10°) vanes $\tilde{\zeta}_{s,orig}$ and new vanes consisting of two parts $\tilde{\zeta}_{s,Va}$ was evaluated from the CFD data for the reverse flow, i.e. $\tilde{\zeta}_{s,orig,rev}$ = 0.061 and $\tilde{\zeta}_{s,Va,\ rev}$= 0.093. The total loss coefficient for the stator row is defined as follows: $\tilde{\zeta}_{s,rev} = (\tilde{p}_{c3} - \tilde{p}_{c2})/(\tilde{p}_{c3} - \tilde{p}_{s3})$. The mass-averaged pressures in the planes located ahead and behind the stator row are denoted by the tilde above a letter. Higher pressure losses, due to the application of the stator vanes that turn in one go, are acceptable due to the fact that the maximum efficiency of the reverse flow is relatively low: $\eta_{max,\ rev}$ = 40 % to 50 %.

Tandem stator vanes

The standard stator vanes have the movable and fixed parts connected by a special locking mechanism. It restricts the flow through the gap between two stator vane parts. Two further variants, denoted as Vb and Vc, of the stator vanes consisting of two parts with the relative peripheral clearance $(\Delta/(c_{S1} + c_{S2}))$ of 10 % and 5 % at the mid-span were designed and are shown in Fig. 8. These stator vane configurations are in fact tandem compressor cascades, refer to [10] and [11], with the relative clearance selected in accordance with recommendations in [10]. Performance curves were calculated using the CFD data; theoretical points for the Vb variant are denoted by red crosses in Figs. 9. The results acquired for the Vc variant are very similar, thus we drew only one point, denoted by green triangle, at the design condition (φ = 0.35). The measured and calculated efficiencies differences for the fan standard run at the design working condition are presented in Table 2. It can be seen that the Vb and Vc variants have lower stage efficiency of 1.5 % and 2.0 % than the standard stator vane variant Va.

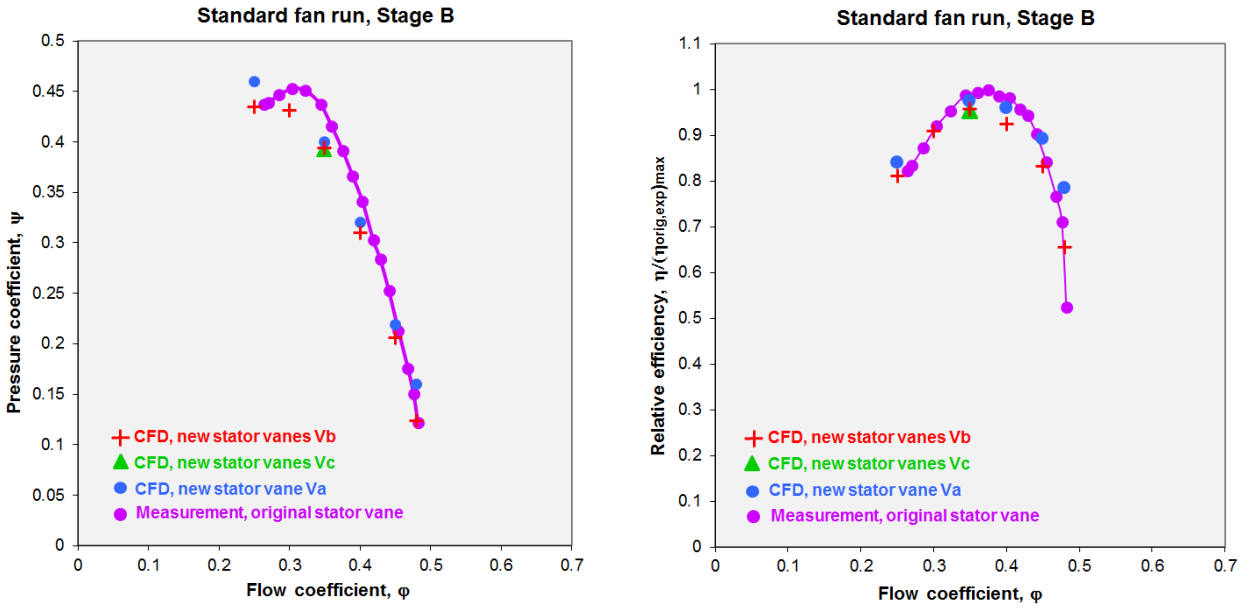

Figure 9: Stage B measured and calculated performance

Table 2: Stage B efficiency, CFD, φ_D = 0.35, standard run

Stator vanes variants	Va	Vb	Vc
Δη (%)	1.2	2.7	3.2
$\tilde{\zeta}_{S,\,i}$	0.060	0.070	0.074

$\Delta\eta = \eta_{ex,orig} - \eta_i$, indexes i = Va, Vb and Vc

The stator total loss coefficient values $\tilde{\zeta}_S$ valid for all variants in the design stage condition (φ = 0.35) are presented in Table No. 2. The coefficient $\tilde{\zeta}_S$ is defined: $\tilde{\zeta}_{s,} = (\tilde{p}_{c2} - \tilde{p}_{c3})/ - (\tilde{p}_{c2} \tilde{p}_{s2})$. The mass-averaged pressures in the planes located ahead and behind the stator row at the fan standard run are denoted by the tilde above a letter.

The maximum flow deviation from the axial direction was $\alpha_3 = 3.5^o$ in the annulus area outside the end-wall boundary layers for all variants of the stator vane row (Va, Vb and Vc), which does not adversely affect the fan's outlet diffuser performance (Fig. 10), e.g. [5]. Stator outlet flow angle α_3 was calculated with help of peripherally averaged velocity components.

Velocity distributions in the mid-span cascades of the 3 stator vane row variants (Va, Vb and Vc) at the standard run of the Stage B are shown in Fig. 11. We can observe the flow jets in the peripheral gaps between the moveable and fixed vane parts in the tandem cascades configurations Vb and Vc. These flow jets are additional source of energy losses, as the boundary layers on the fixed vane parts are not essentially affected. The maximum velocity area near the inlet of the movable curved vane part for the basic variant Va is smaller than in the Vb and Vc variants with gaps. Higher velocity gradients in the said variants contribute to the higher energy losses. Our findings are in agreement with the stator row total loss coefficients values $\tilde{\zeta}_S$, shown in Table No. 2.

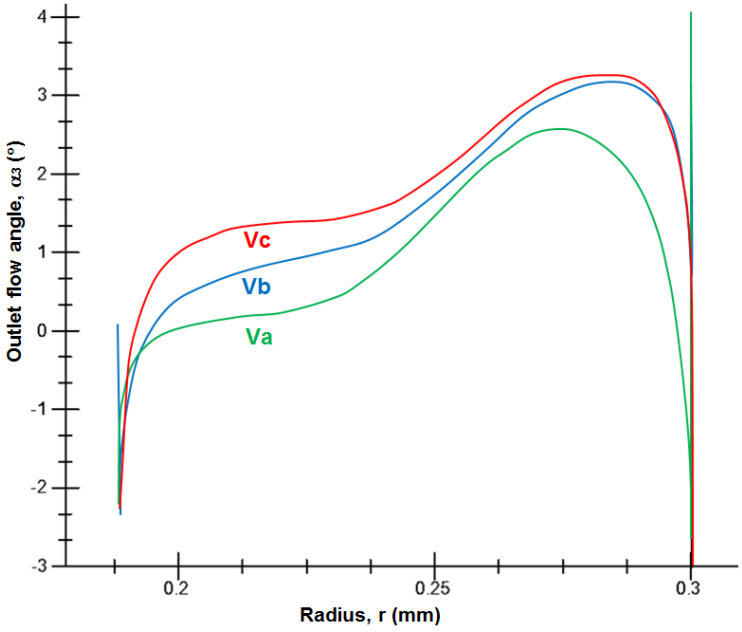

Figure 10: Stage B spanwise distribution of stator outlet flow angle

CONCLUSION

Fan flow directional change is frequently required in ventilation systems during emergencies in traffic tunnels, coalmines or miscellaneous chemical plant production lines. Axial flow fans are used. The flow reversal is usually carried out by changing the direction of rotation and by turning the stator vanes. Companies that procure reverse axial fans require that the stator vanes will have the capability of turning in one go around their axis in emergency events to enable the reverse flow. Consequently, new stator vanes were designed for the two axial fan stages, namely A and B, with different cascade aerodynamic loading. Our main findings may be summarised as follows:

i) Fan hub is subjected to the highest aerodynamic loading of stator blade elements, if the stage blading is designed in accordance with the free-vortex law. The flow without large separation area will take place in the stator row with rotating vanes near the hub, if the diffusion factor D is less than the safe limit $D < 0.56$ and the inlet flow angle $\alpha_2 < 40^o$.

ii) The comparison of results between the computed and measured performance of Stages A and B is acceptable at the standard fan run. Consequently, the effect of the stator vane design

options for turning in one go (reversing) on the fan performance was investigated in relation to the Stage A and B efficiency computed with the use of flow simulation data.

iii) Stage A with moderate loading of the stator cascade can use vanes that rotate around their axis, where the ratio of spacing and chord of cascade s/c is higher than 1.02 along the full span.

iv) Application of the Stage A turning vanes causes decrease in the stage efficiency by 0.5 % at the design working condition.

v) Stage B with higher aerodynamic loading has the inlet flow angle α_2 of 47^o on the stator hub. As a result, the application of turning stator vanes is not feasible and special vanes designed by authors may be used instead. The stator vane (Va) consists of two parts, fixed straight part and moveable curved part, which during the standard flow are connected. During the reverse flow, the moveable curved stator blade part is turned to ensure the maximum flow rate.

vi) Two further Stage B variants, denoted as Vb and Vc, of the stator vanes consisting of two parts, namely tandem stator vanes with the relative peripheral clearance of 10 % and 5 % at the mid-span were designed. Use of the tandem vanes causes decrease in the stage efficiency of 1.5 % and 2.0 % at the design working condition when compared with the standard variant Va.

vii) We concluded that the application of newly designed reverse axial fan Stage A and B with turning stator vanes and vanes consisting of two parts that have the capability to turn in one go at the flow reversal is acceptable. Further research in the reverse axial flow fan aerodynamics is recommended.

ACKNOWLEDGEMENT

Our study was carried out for ZVVZ Machinery and was sponsored by grants by the Czech Technology Agency (TACR; No. TA04020228) and the Czech Ministry of Trade and Industry (No. TIP FR-TI1/347). Authors were pleased to receive the said grants and wish to express their thanks.

BIBLIOGRAPHY

[1] I.V. Brusilovskij – *Aerodinamičeskij rasčot osevych ventilatorov (Aerodynamic Design of Axial Fans)*, Mašinostrojenije, Moscow, **1986**

[2] V. Cyrus – *Axial Fan at Reversal Flow*, ASME Paper No. GT 2004 – 53446, Vienna, June 14-17, **2004**

[3] V. Cyrus, J. Pelnar and J. Cyrus – *Reversing of Axial Fans for Ventilation*, ASME Paper No. GT 20114-6062, Vancouver, June 6-10, **2011**

[4] S. Lieblein – *Experimental Flow in Two-Dimensional Cascades*, NASA SP 36, p. 183, **1965**

[5] N. Cumpsty – *Compressor Aerodynamics*, Krieger Publishing Company. Malabar, **2004**

[6] V. Cyrus – *An Experimental Study of Stall in Four Axial Compressor Stages*, ASME Paper No. 2000 GT – 504, Munich, June **2000**

[7] V. Cyrus V., V. Bruna, V. Folta , P. Kolar, M. Lindova et al – *Program Package for Design of Axial Flow Compressor Stage*, Internal technical reports of SVUSS and AHT Energetika

[8] FINE™/Turbo Numeca Code, Manuals, **2015**

[9] V. Cyrus – AHT Energetika: CR Patent No. 306953, **2017**

[10] J. P. Gostellow – *Cascade Aerodynamics*, Pergamon Press, Oxford, **1984**

[11] J. M. Glumphy – *Numerical Investigation of Subsonic Axial Flow Tandem Airfoils for a Core Compressor Rotor*, Ph. D. Thesis, Virginia Polytechnic Institute, **2008**

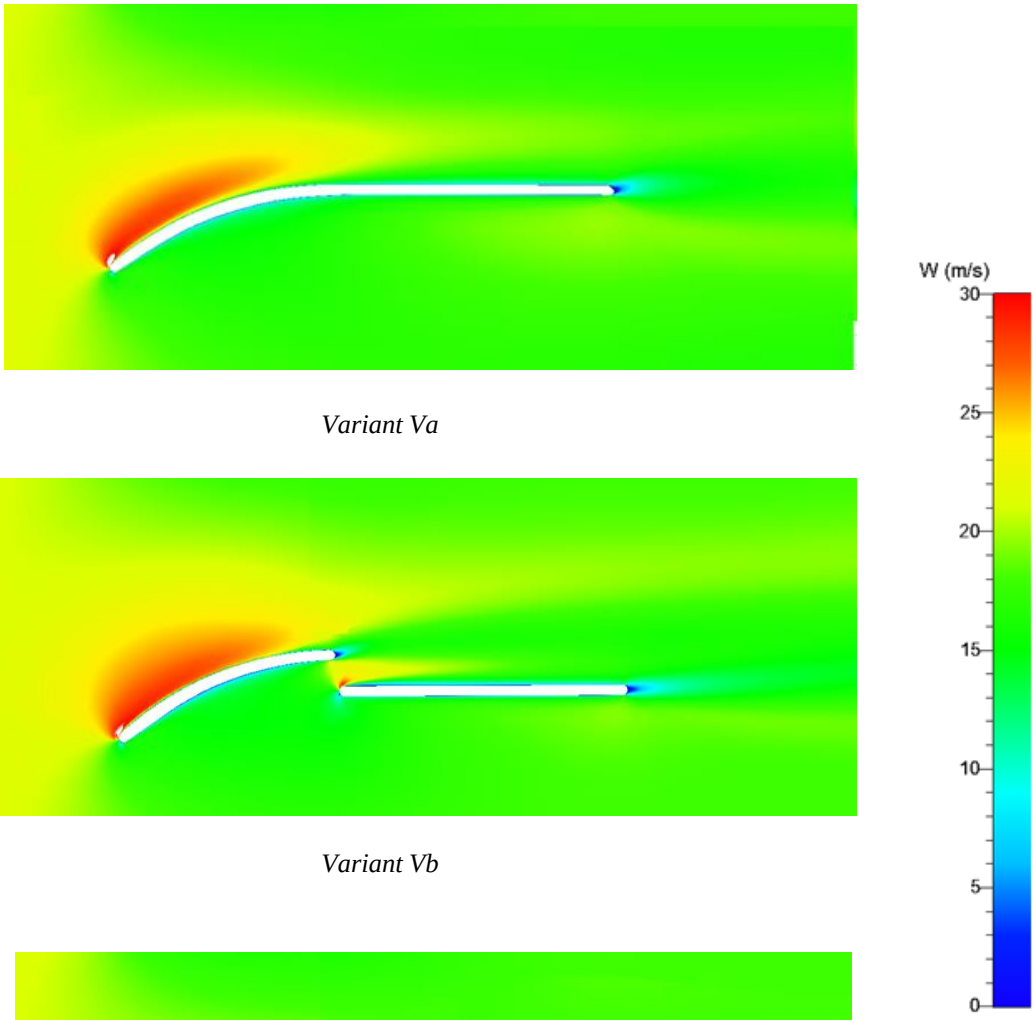

Variant Va

Variant Vb

Variant Vc

Figure 11: Velocity distributions in the mid-span of Stage B stator cascades